

Effect of Extended Gravitational Decoupling on Isotropization and Complexity in $f(\mathbb{R}, \mathbb{T})$ Theory

M. Sharif¹ *and Tayyab Naseer^{1,2} †

¹ Department of Mathematics and Statistics, The University of Lahore, 1-KM Defence Road Lahore, Pakistan.

² Department of Mathematics, University of the Punjab, Quaid-i-Azam Campus, Lahore-54590, Pakistan.

Abstract

This paper develops some new analytical solutions to the $f(\mathbb{R}, \mathbb{T})$ field equations through extended gravitational decoupling. For this purpose, we take spherical anisotropic configuration as a seed source and extend it to an additional source. The modified field equations comprise the impact of both sources which are then decoupled into two distinct sets by applying the transformations on g_{tt} and g_{rr} metric potentials. The original anisotropic source is adorned by the first sector, and we make it solvable by considering two different well-behaved solutions. The second sector is in terms of an additional source and we adopt some constraints to find deformation functions. The first constraint is the isotropization condition which transforms the total fluid distribution into an isotropic system only for a specific value of the decoupling parameter. The other constraint is taken as the complexity-free fluid distribution. The unknown constants are calculated at the hypersurface through matching conditions. The preliminary information (mass and radius) of a compact star $4U1820 - 30$ is employed to analyze physical attributes of the resulting models. We conclude that

*msharif.math@pu.edu.pk

†tayyabnaseer48@yahoo.com

certain values of both the coupling as well as decoupling parameter yield viable and stable solutions in this theory.

Keywords: $f(\mathbb{R}, \mathbb{T})$ gravity; Anisotropy; Self-gravitating systems; Gravitational decoupling.

PACS: 04.50.Kd; 04.40.Dg; 04.40.-b.

1 Introduction

The well-structured but perplexing composition of our cosmos includes massive geometrical bodies such as stars, clusters and other mysterious constituents. Since the universe has passed through different epochs, its evolution has become a topic of great interest for astrophysicists. The cosmos, in which we are living, is going through a very special era, i.e., it is currently expanding with an acceleration rate. Cosmologists confirmed such expansion by performing several attempts on distant galaxies. It is claimed that an abundance of a mysterious force with large repulsive pressure (known as the dark energy) causes this rapid expansion. General relativity (\mathbb{GR}) is the first ever theory which helps researchers to figure out both cosmological and astrophysical phenomena properly. However, this theory faces two major drawbacks (cosmic coincidence and fine-tuning), and thus its multiple extensions have recently been introduced to tackle with these issues. The $f(\mathbb{R})$ theory is the simplest extension to \mathbb{GR} which was obtained by putting generic function of the Ricci scalar in place of \mathbb{R} in an Einstein-Hilbert action. Various authors [1, 2] discussed this theory to explain inflationary as well as present eras. The regions in which multiple $f(\mathbb{R})$ models show stable behavior have been discussed with the help of different techniques [3, 4].

The concept of matter-geometry interaction in $f(\mathbb{R})$ framework was introduced by Bertolami et al. [5] for the very first time. They added the role of geometrical quantity \mathbb{R} in the Lagrangian \mathbb{L}_m and analyzed how physical features of celestial bodies vary. After this, many people put their attention to generalize such couplings at some action level which may help in figuring out cosmic accelerated expansion. Harko et al. [6] developed $f(\mathbb{R}, \mathbb{T})$ theory, in which \mathbb{T} expresses trace of the energy-momentum tensor (\mathbb{EMT}) whose inclusion yields new gravitational aspects. The role of minimal as well as non-minimal interaction on test particles can be studied through different models of this gravity. There exists an additional force (depends on density and pressure [7]) due to the non-conserved nature of the corresponding

EMT in this theory. A minimal $f(\mathbb{R}, \mathbb{T})$ model has been employed to explain switching of the matter-dominated epoch into late-time acceleration era [8]. A particular $\mathbb{R} + 2\varpi\mathbb{T}$ model has widely been used by researchers through which several noteworthy results are obtained. Das et al. [9] studied gravastar model with three different equations of state, representing its inner, intermediate and outer regions in this theory. Deb et al. [10] explored strange star with isotropic distribution and obtained acceptable behavior of the developed solution. Various authors [11, 12] labeled this theory as the best approach to discuss stellar interiors.

The non-linear nature of the field equations describing a self-gravitating object makes it much difficult to solve them analytically. It has always been interesting to calculate well-behaved solutions of such complicated equations and study physical feasibility of realistic systems. In this regard, a large body of literature is stuffed with solutions which have been formulated through multiple techniques. The gravitational decoupling is one of the recently developed techniques to formulate feasible solutions analogous to the fluid distribution involving multiple sources (such as anisotropy, dissipation flux and shear). The minimal geometric deformation (MGD) was firstly developed by Ovalle [13] in the context of braneworld to find exact solutions representing compact models. Later on, Ovalle et al. [14] employed this strategy to calculate extended solutions from the seed isotropic domain and observed their nature through graphical analysis. Sharif and Sadiq [15] determined two exact solutions corresponding to charged sphere in \mathbb{GR} through which the influence of electromagnetic field was observed on them. An isotropic solution was extended into multiple anisotropic models in $f(\mathbb{G})$ and $f(\mathbb{R})$ frameworks [16].

Estrada and Tello-Ortiz [17] developed some stable models by extending the domain of isotropic Heintzmann solution in this framework. Hensh and Stuchlik [18] found that modified Tolman VII solution entails pressure anisotropy on which the influence of decoupling parameter is also observed. The MGD approach has proved to be successful in obtaining analytical solutions, however it has a drawback, i.e., it does not explain a black hole structure with a well-defined horizon. As a result, Ovalle [19] deformed both the metric components, and thus named it as the extended geometric deformation (EGD). Contreras and Bargueño [20] assumed vacuum BTZ ansatz and extended it to exterior charged BTZ solution by means of EGD. Sharif and his collaborators [21] constructed multiple acceptable extensions in \mathbb{GR} , $f(\mathbb{R})$ and Brans-Dicke theories. Zubair et al. [22] formulated the extended

charged Heintzmann solutions and found them stable for specific values of the decoupling parameter. We have analyzed the role of matter-geometry coupling on several anisotropic compact models [23].

The notion of complexity in self-gravitating systems has been recognized as an interesting topic in the last few years. Researchers developed multiple definitions in such a way that the parameters defining complexity of the physical structure can completely describe that system but found them inadequate. In this regard, the most appropriate definition was recently established for the case of static sphere [24] and then extended to the dynamical matter source [25]. It was found that the orthogonal decomposition of the curvature tensor yields some scalars incorporating different physical attributes such as the inhomogeneous energy density and local anisotropy. This idea has been extended for static/dynamical configurations in modified framework [26, 27]. The complexity-free condition can be used as a constraint to solve the complicated field equations. This constraint has been used to formulate acceptable solutions through decoupling scheme [28]. Casadio et al. [29] applied MGD strategy on the field equations and calculated their solutions corresponding to the isotropization as well as complexity-free conditions. Maurya et al. [30] explored the impact of decoupling parameters on both these solutions with the help of MGD and EGD. Sharif and Majid [31] adopted two different forms of metric components to extend this work in the context of Brans-Dicke theory and found physically feasible models.

This paper explores the effect of $f(\mathbb{R}, \mathbb{T})$ gravity on two different decoupled solutions representing static spherically symmetric interior distribution. We firstly isotropize the system by considering the vanishing anisotropy for $\beta = 1$, and obtain the corresponding solution. We then formulate the other solution by using the complexity dependent constraint, i.e., total matter source with zero complexity. The paper has the following format. In the next section, we discuss some basic quantities and the modified field equations influenced from additional source. We then apply EGD scheme to decouple these equations in section 3. We formulate two solutions corresponding to the above constraints in sections 4 and 5. The graphical interpretation of physical features is given in section 6. Finally, we conclude our results in section 7.

2 The $f(\mathbb{R}, \mathbb{T})$ Theory

The inclusion of an additional field along with the modified functional in the Einstein-Hilbert action (with $\kappa = 8\pi$) yields [6]

$$S_{f(\mathbb{R}, \mathbb{T})} = \int \frac{1}{16\pi} [f(\mathbb{R}, \mathbb{T}) + \mathbb{L}_m + \beta\mathbb{L}_{\mathfrak{B}}] \sqrt{-g} d^4x, \quad (1)$$

where the Lagrangian corresponding to the seed and additional sources are represented by \mathbb{L}_m and $\mathbb{L}_{\mathfrak{B}}$, respectively. Here, the influence of an extra source (gravitationally coupled to the original source) on self-gravitating system is controlled by the decoupling parameter β . The variation of the action (1) with respect to $g_{\eta\zeta}$ provides the field equations in modified gravity as

$$\mathbb{G}_{\eta\zeta} = 8\pi \mathbb{T}_{\eta\zeta}^{(Tot)}, \quad (2)$$

where the Einstein tensor $\mathbb{G}_{\eta\zeta}$ describes geometry of the considered structure whereas the matter configuration is characterized by right hand side which can further be classified as

$$\mathbb{T}_{\eta\zeta}^{(Tot)} = \mathbb{T}_{\eta\zeta}^{(Eff)} + \beta\mathfrak{B}_{\eta\zeta} = \frac{1}{f_{\mathbb{R}}} \mathbb{T}_{\eta\zeta} + \mathbb{T}_{\eta\zeta}^{(D)} + \beta\mathfrak{B}_{\eta\zeta}. \quad (3)$$

Here, $\mathfrak{B}_{\eta\zeta}$ is a newly added source and $\mathbb{T}_{\eta\zeta}^{(Eff)}$ is the effective EMT of $f(\mathbb{R}, \mathbb{T})$ theory. The modified sector $\mathbb{T}_{\eta\zeta}^{(D)}$ of this gravity has the form

$$\begin{aligned} \mathbb{T}_{\eta\zeta}^{(D)} &= \frac{1}{8\pi f_{\mathbb{R}}} \left[f_{\mathbb{T}} \mathbb{T}_{\eta\zeta} + \left\{ \frac{1}{2} (f - \mathbb{R} f_{\mathbb{R}}) - \mathbb{L}_m f_{\mathbb{T}} \right\} g_{\zeta\eta} \right. \\ &\quad \left. + (\nabla_{\eta} \nabla_{\zeta} - g_{\eta\zeta} \square) f_{\mathbb{R}} + 2f_{\mathbb{T}} g^{\rho\alpha} \frac{\partial^2 \mathbb{L}_m}{\partial g^{\eta\zeta} \partial g^{\rho\alpha}} \right], \end{aligned} \quad (4)$$

where $f_{\mathbb{T}} = \frac{\partial f(\mathbb{R}, \mathbb{T})}{\partial \mathbb{T}}$ and $f_{\mathbb{R}} = \frac{\partial f(\mathbb{R}, \mathbb{T})}{\partial \mathbb{R}}$. Furthermore, $\square \equiv \frac{1}{\sqrt{-g}} \partial_{\eta} (\sqrt{-g} g^{\eta\zeta} \partial_{\zeta})$ and ∇_{η} symbolize the D'Alembert operator and covariant derivative, respectively.

The nature of the original (seed) fluid distribution is assumed to be anisotropic which can be characterized by the EMT given as

$$\mathbb{T}_{\eta\zeta} = (\mu + P_{\perp}) \mathcal{K}_{\eta} \mathcal{K}_{\zeta} + (P_r - P_{\perp}) \mathcal{W}_{\eta} \mathcal{W}_{\zeta} + P_{\perp} g_{\eta\zeta}, \quad (5)$$

where μ is the energy density, P_r and P_\perp are the radial/tangential pressures. Also, \mathcal{W}_η and \mathcal{K}_η are treated as the four-vector and four-velocity, respectively. One can determine the trace of $f(\mathbb{R}, \mathbb{T})$ field equations as follows

$$3\nabla^\eta \nabla_\eta f_{\mathbb{R}} + 4f_{\mathbb{T}} \mathbb{L}_m + \mathbb{R} f_{\mathbb{R}} - 2f - \mathbb{T}(f_{\mathbb{T}} + 1) - 2g^{\eta\zeta} g^{\rho\alpha} f_{\mathbb{T}} \frac{\partial^2 \mathbb{L}_m}{\partial g^{\eta\zeta} \partial g^{\rho\alpha}} = 0.$$

The results of $f(\mathbb{R})$ gravity can be recovered for the case when $f_{\mathbb{T}} = 0$. As this theory involves the interaction between geometry and matter, thus the covariant divergence of the corresponding EMT is non-null. Consequently, there appears an additional force in the gravitational field of massive structures. Thus we obtain

$$\nabla^\eta \mathbb{T}_{\eta\zeta} = \frac{f_{\mathbb{T}}}{8\pi - f_{\mathbb{T}}} \left[\nabla^\eta \Theta_{\eta\zeta} + (\mathbb{T}_{\eta\zeta} + \Theta_{\eta\zeta}) \nabla^\eta \ln f_{\mathbb{T}} - \frac{8\pi\beta}{f_{\mathbb{T}}} \nabla^\eta \mathfrak{B}_{\eta\zeta} - \frac{1}{2} g_{\rho\alpha} \nabla_\zeta \mathbb{T}^{\rho\alpha} \right], \quad (6)$$

where $\Theta_{\eta\zeta} = -2\mathbb{T}_{\eta\zeta} + g_{\eta\zeta} \mathbb{L}_m - 2g^{\rho\alpha} \frac{\partial^2 \mathbb{L}_m}{\partial g^{\eta\zeta} \partial g^{\rho\alpha}}$ and \mathbb{L}_m is considered to be $P = \frac{P_r + 2P_\perp}{3}$ in this case leading to $\frac{\partial^2 \mathbb{L}_m}{\partial g^{\eta\zeta} \partial g^{\rho\alpha}} = 0$.

The geometry of spacetime structure contains two regions, namely inner and outer which are distinguished by the hypersurface Σ , thus the interior of static spherical system is defined by the following metric

$$ds^2 = -e^\chi dt^2 + e^\sigma dr^2 + r^2 d\theta^2 + r^2 \sin^2 \theta d\vartheta^2, \quad (7)$$

where $\chi = \chi(r)$ and $\sigma = \sigma(r)$. The terms \mathcal{W}^η and \mathcal{K}^η for this line element are calculated as

$$\mathcal{W}^\eta = (0, e^{\frac{-\sigma}{2}}, 0, 0), \quad \mathcal{K}^\eta = (e^{\frac{-\chi}{2}}, 0, 0, 0), \quad (8)$$

satisfying the relations

$$\mathcal{W}^\eta \mathcal{W}_\eta = 1, \quad \mathcal{W}^\eta \mathcal{K}_\eta = 0, \quad \mathcal{K}^\eta \mathcal{K}_\eta = -1.$$

We adopt a particular $f(\mathbb{R}, \mathbb{T})$ model to make our results meaningful. The structural transformation of spherical objects can entirely be discussed by taking the linear model as follows

$$f(\mathbb{R}, \mathbb{T}) = f_1(\mathbb{R}) + 2f_2(\mathbb{T}) = \mathbb{R} + 2\varpi\mathbb{T}, \quad (9)$$

with $f_2(\mathbb{T}) = \varpi\mathbb{T}$, ϖ is a real-valued coupling parameter and $\mathbb{T} = 2P_\perp + P_r - \mu$. Houndjo and Piattella [32] observed that the holographic dark energy

features may be discussed through model (9) while exploring the pressureless fluid configuration. The standard conservation of the EMT is also observed to be compatible with this model [33].

The field equations analogous to spherical self-gravitating system (7) and modified model (9) are

$$e^{-\sigma} \left(\frac{\sigma'}{r} - \frac{1}{r^2} \right) + \frac{1}{r^2} = 8\pi (\mu - \beta \mathfrak{B}_0^0) + \frac{\varpi}{3} (9\mu - P_r - 2P_\perp), \quad (10)$$

$$e^{-\sigma} \left(\frac{1}{r^2} + \frac{\chi'}{r} \right) - \frac{1}{r^2} = 8\pi (P_r + \beta \mathfrak{B}_1^1) - \frac{\varpi}{3} (3\mu - 7P_r - 2P_\perp), \quad (11)$$

$$\frac{e^{-\sigma}}{4} \left\{ 2\chi'' + \chi'^2 - \sigma'\chi' + \frac{2(\chi' - \sigma')}{r} \right\} = 8\pi (P_\perp + \beta \mathfrak{B}_2^2) - \frac{\varpi}{3} (3\mu - P_r - 8P_\perp), \quad (12)$$

where the factors multiplied with ϖ appear due to the modified theory and prime means $\frac{\partial}{\partial r}$. Moreover, Eq.(6) after some manipulation yields

$$\begin{aligned} \frac{dP_r}{dr} + \frac{\chi'}{2} (\mu + P_r) + \frac{\beta\chi'}{2} (\mathfrak{B}_1^1 - \mathfrak{B}_0^0) + \frac{2}{r} (P_r - P_\perp) \\ + \beta \frac{d\mathfrak{B}_1^1}{dr} + \frac{2\beta}{r} (\mathfrak{B}_1^1 - \mathfrak{B}_2^2) = -\frac{\varpi}{4\pi - \varpi} (\mu' - P'), \end{aligned} \quad (13)$$

where the term on the right hand side reveals non-conserved nature of $f(\mathbb{R}, \mathbb{T})$ theory. The variations in the structure of any self-gravitating body can be studied through Eq.(13) which is also identified as the generalized Tolman-Opphenheimer-Volkoff equation. The unknowns are now increased as the additional source is incorporated in the field equations. These unknowns are χ , σ , μ , P_r , P_\perp , \mathfrak{B}_0^0 , \mathfrak{B}_1^1 and \mathfrak{B}_2^2 , thus the only possibility to obtain analytic solution is the consideration of some constraints. In this regard, we use an efficient approach [14] to obtain solutions for the considered setup.

3 Gravitational Decoupling

A systematic approach which allows both the temporal as well as radial metric potentials to be transformed to get solutions of the field equations is known as the extended gravitational decoupling. We employ this scheme to decouple the field equations so that we can solve each sector separately. We

assume the following solution of Eqs.(10)-(12) to implement this technique as

$$ds^2 = -e^{\xi(r)} dt^2 + \frac{1}{\rho(r)} dr^2 + r^2 d\theta^2 + r^2 \sin^2 \theta d\vartheta^2. \quad (14)$$

The linear transformations on temporal and radial metric coefficients are of the form

$$\xi \rightarrow \chi = \xi + \beta \mathcal{G}, \quad \rho \rightarrow e^{-\sigma} = \rho + \beta \mathcal{F}, \quad (15)$$

where $\mathcal{G} = \mathcal{G}(r)$ and $\mathcal{F} = \mathcal{F}(r)$ are the temporal and radial deformation functions, respectively. It is worth noting that these linear mappings do not disturb the spherical symmetry. The set representing seed (anisotropic) source can be separated from the field equations (10)-(12) by implementing the transformations (15) (for $\beta = 0$) as

$$e^{-\sigma} \left(\frac{\sigma'}{r} - \frac{1}{r^2} \right) + \frac{1}{r^2} = 8\pi\mu + \frac{\varpi}{3} (9\mu - P_r - 2P_\perp), \quad (16)$$

$$e^{-\sigma} \left(\frac{1}{r^2} + \frac{\chi'}{r} \right) - \frac{1}{r^2} = 8\pi P_r - \frac{\varpi}{3} (3\mu - 7P_r - 2P_\perp), \quad (17)$$

$$\frac{e^{-\sigma}}{4} \left(\chi'^2 - \sigma' \chi' + 2\chi'' - \frac{2\sigma'}{r} + \frac{2\chi'}{r} \right) = 8\pi P_\perp - \frac{\varpi}{3} (3\mu - P_r - 8P_\perp), \quad (18)$$

which yield the explicit expressions of the state variables as

$$\begin{aligned} \mu &= \frac{e^{-\sigma}}{48r^2(\varpi + 2\pi)(\varpi + 4\pi)} [2\{r^2\varpi\chi'' + 8r\sigma'(\varpi + 3\pi) + 8(\varpi + 3\pi) \\ &\quad \times (e^\sigma - 1)\} + r^2\varpi\chi'^2 + r\varpi\chi'(4 - r\sigma')], \end{aligned} \quad (19)$$

$$\begin{aligned} P_r &= \frac{e^{-\sigma}}{48r^2(\varpi + 2\pi)(\varpi + 4\pi)} [2\{4r\varpi\sigma' - r^2\varpi\chi'' - 8(\varpi + 3\pi)(e^\sigma - 1)\} \\ &\quad - r^2\varpi\chi'^2 + r\sigma'(20\varpi + r\varpi\sigma' + 48\pi)], \end{aligned} \quad (20)$$

$$\begin{aligned} P_\perp &= \frac{e^{-\sigma}}{48r^2(\varpi + 2\pi)(\varpi + 4\pi)} [10r^2\varpi\chi'' + (5\varpi + 12\pi)r^2\chi'^2 + 24\pi r^2\chi'' \\ &\quad - 8\varpi + r\chi'\{8(\varpi + 3\pi) - (5\varpi + 12\pi)r\sigma'\} - 4r\sigma'(\varpi + 6\pi) + 8\varpi e^\sigma]. \end{aligned} \quad (21)$$

Another set characterizing the role of additional source ($\mathfrak{B}_{\eta\zeta}$) is obtained for $\beta = 1$ as

$$8\pi\mathfrak{B}_0^0 = \frac{1}{r} \left(\mathcal{F}' + \frac{\mathcal{F}}{r} \right), \quad (22)$$

$$8\pi\mathfrak{B}_1^1 = \frac{\mathcal{F}}{r} \left(\chi' + \frac{1}{r} \right) + \frac{e^{-\sigma}\mathcal{G}'}{r}, \quad (23)$$

$$8\pi\mathfrak{B}_2^2 = \frac{\mathcal{F}}{4} \left(2\chi'' + \chi'^2 + \frac{2\chi'}{r} \right) + \frac{\mathcal{F}'}{4} \left(\chi' + \frac{2}{r} \right) + \frac{e^{-\sigma}}{2} \left(\mathcal{G}'' + \chi'\mathcal{G}' + \frac{\beta\mathcal{G}'^2}{2} + \frac{\mathcal{G}'}{r} - \frac{\sigma'\mathcal{G}'}{2} \right). \quad (24)$$

The EGD scheme allows the two (seed and newly added) matter distributions to exchange energy between them. Both of these sources are not conserved individually but the system becomes conserved by coupling them into a single framework. A successful partition of the system (10)-(12) has now been done into two sets. For the case of first set, we have three equations (19)-(21) along with five unknown quantities $(\mu, P_r, P_\perp, \chi, \sigma)$, so we will assume a well-behaved solution to make this system solvable. The other set (22)-(24) comprises of five unknowns $(\mathcal{G}, \mathcal{F}, \mathfrak{B}_0^0, \mathfrak{B}_1^1, \mathfrak{B}_2^2)$, thus two constraints on \mathfrak{B} -sector will be required at the same time to close the system. We define the effective state variables as follows

$$\check{\mu} = \mu - \beta\mathfrak{B}_0^0, \quad \check{P}_r = P_r + \beta\mathfrak{B}_1^1, \quad \check{P}_\perp = P_\perp + \beta\mathfrak{B}_2^2, \quad (25)$$

and the total anisotropy is

$$\check{\Pi} = \check{P}_\perp - \check{P}_r = (P_\perp - P_r) + \beta(\mathfrak{B}_2^2 - \mathfrak{B}_1^1) = \Pi + \Pi_{\mathfrak{B}}, \quad (26)$$

where Π and $\Pi_{\mathfrak{B}}$ are anisotropic factors corresponding to the seed and new source, respectively.

4 Isotropization of Compact Sources

We can observe from Eq.(26) that there may be a difference between anisotropic factors generated by the original source $\mathbb{T}_{\zeta\eta}$ and the total matter distribution, i.e., Π and $\check{\Pi}$, respectively. In this sector, we assume that the incorporation of new source in the original anisotropic source makes it an isotropic which means $\check{\Pi} = 0$. This variation in spherical system is controlled by parameter β , since $\beta = 0$ specifies anisotropic distribution and 1 represents an isotropic one. We now discuss the later case in order to isotropize the system which gives

$$\Pi_{\mathfrak{B}} = -\Pi \quad \Rightarrow \quad \mathfrak{B}_2^2 - \mathfrak{B}_1^1 = P_r - P_\perp. \quad (27)$$

Casadio et al. [29] considered a self-gravitating system comprising anisotropic distribution at some initial time and then used the constraint (27) to convert it into an isotropic configuration through gravitational decoupling. As we have mentioned earlier, we are required to take a solution associated with the original source to construct our solution, thus we have

$$\chi(r) = \ln \left\{ \mathcal{A}^2 \left(1 + \frac{r^2}{\mathcal{B}^2} \right) \right\}, \quad (28)$$

$$\rho(r) = e^{-\sigma} = \frac{\mathcal{B}^2 + r^2}{\mathcal{B}^2 + 3r^2}, \quad (29)$$

$$\mu = \frac{3\mathcal{B}^2(3\varpi + 8\pi) + 2r^2(5\varpi + 12\pi)}{4(\mathcal{B}^2 + 3r^2)^2(\varpi + 4\pi)(\varpi + 2\pi)}, \quad (30)$$

$$P_r = \frac{\varpi(3\mathcal{B}^2 + 2r^2)}{4(\mathcal{B}^2 + 3r^2)^2(\varpi + 4\pi)(\varpi + 2\pi)}, \quad (31)$$

$$P_{\perp} = \frac{3\varpi\mathcal{B}^2 + 4r^2(2\varpi + 3\pi)}{4(\mathcal{B}^2 + 3r^2)^2(\varpi + 4\pi)(\varpi + 2\pi)}, \quad (32)$$

where we employ matching criteria to calculate the unknowns, i.e., \mathcal{A}^2 and \mathcal{B}^2 . When a cluster of test particles moves in circular orbit in any gravitational field, the above solution may help to determine that field [34]. This form of metric potentials has also been employed in \mathbb{GR} to develop decoupled solutions [29].

Some constraints play a significant role in the study of various characteristics of self-gravitating bodies, known as junction conditions that provide solutions at the hypersurface ($\Sigma : r = \mathcal{R}$). To discuss the matching conditions, we take the most appropriate choice of exterior geometry, i.e., the Schwarzschild metric. The inclusion of higher-order curvature terms in $f(\mathbb{R})$ gravity (like the Starobinsky model given by $\mathbb{R} + \alpha\mathbb{R}^2$, where α is a restricted constant) make the junction conditions different from that in \mathbb{GR} [35, 36]. However, for the case of model (9), the first term represents \mathbb{GR} and the second entity does not contribute to the current setup. Therefore, the exterior geometry is taken as that of \mathbb{GR} by

$$ds^2 = -\frac{r - 2\check{\mathcal{M}}}{r} dt^2 + \frac{r}{r - 2\check{\mathcal{M}}} dr^2 + r^2 d\theta^2 + r^2 \sin^2 \theta d\varphi^2, \quad (33)$$

where $\check{\mathcal{M}}$ is the total mass. This provides after matching with interior spher-

ical geometry (7) as

$$\mathcal{A}^2 = \frac{\mathcal{R} - 2\check{\mathcal{M}}}{\frac{\check{\mathcal{M}}\mathcal{R}}{\mathcal{R} - 3\check{\mathcal{M}}} + \mathcal{R}}, \quad (34)$$

$$\mathcal{B}^2 = \frac{\mathcal{R}^2(\mathcal{R} - 3\check{\mathcal{M}})}{\check{\mathcal{M}}}. \quad (35)$$

Further, the graphical interpretation of different physical features will be studied by using mass ($\check{\mathcal{M}} = 1.58 \pm 0.06 M_{\odot}$) and radius ($\mathcal{R} = 9.1 \pm 0.4 km$) of $4U1820 - 30$ star model [37]. Using the constraint (27) and modified field equations, we obtain a non-linear differential equation in terms of metric functions (28)-(29) as

$$\begin{aligned} & r(\mathcal{B}^2 + r^2) [(\mathcal{B}^2 + r^2) \{2r((\varpi + 4\pi)(\mathcal{B}^4 + 4\mathcal{B}^2 r^2 + 3r^4)\mathcal{G}''(r) + 24\pi r^2) \\ & + (\varpi + 4\pi)r(\mathcal{B}^4 + 4\mathcal{B}^2 r^2 + 3r^4)\mathcal{G}'(r)^2 - 2(\varpi + 4\pi)(\mathcal{B}^4 + 4\mathcal{B}^2 r^2 - 3r^4) \\ & \times \mathcal{G}'(r)\} + 2(\varpi + 4\pi)(\mathcal{B}^2 + 2r^2)(\mathcal{B}^2 + 3r^2)^2 \mathcal{F}'(r)] - 4(\mathcal{B}^2 + 3r^2)^2 \\ & \times (\varpi + 4\pi)(\mathcal{B}^4 + 2\mathcal{B}^2 r^2 + 2r^4)\mathcal{F}(r) = 0. \end{aligned} \quad (36)$$

This is the first and second order in $\mathcal{F}(r)$ and $\mathcal{G}(r)$, respectively. To solve this equation for $\mathcal{F}(r)$ is an easy task, thus we take $\mathcal{G}(r) = gr^2$ with g as a constant. After substituting this in Eq.(36), the analytic solution takes the form

$$\begin{aligned} \mathcal{F}(r) = & \frac{r^2(\mathcal{B}^2 + r^2)}{\mathcal{B}^2 + 2r^2} \left[\mathbb{C}_1 - \frac{1}{9(\varpi + 4\pi)} \left\{ (\varpi + 4\pi)g^2(\mathcal{B}^2 + 3r^2) + 2g \right. \right. \\ & \left. \left. \times (\varpi + 4\pi)(\mathcal{B}^2 g + 3) \ln(\mathcal{B}^2 + 3r^2) + \frac{6(\varpi\mathcal{B}^2 g + \pi(4\mathcal{B}^2 g - 6))}{\mathcal{B}^2 + 3r^2} \right\} \right], \end{aligned} \quad (37)$$

where \mathbb{C}_1 is an integration constant.

The deformed temporal and radial metric components (15) now become

$$e^x = \mathcal{A}^2 e^{\beta g r^2} \left(1 + \frac{r^2}{\mathcal{B}^2} \right), \quad (38)$$

$$\begin{aligned} e^\sigma = \rho^{-1} = & 9(\mathcal{B}^2 + 2r^2)(\mathcal{B}^2 + 3r^2) \left[\beta r^2(\mathcal{B}^2 + r^2) \left\{ 9\mathbb{C}_1(\mathcal{B}^2 + 3r^2) \right. \right. \\ & \left. \left. - g^2(\mathcal{B}^2 + 3r^2)^2 - 2g(\mathcal{B}^2 + 3r^2)(\mathcal{B}^2 g + 3) \ln(\mathcal{B}^2 + 3r^2) - 6\mathcal{B}^2 g \right\} \right] \end{aligned}$$

$$+ \frac{36\pi}{\varpi + 4\pi} \left. \right\} + 9(\mathcal{B}^2 + r^2)(\mathcal{B}^2 + 2r^2) \left. \right]^{-1}. \quad (39)$$

Hence, the extended gravitationally decoupled solution representing the sphere (10)-(12) is given by the following metric as

$$ds^2 = -\mathcal{A}^2 e^{\beta g r^2} \left(1 + \frac{r^2}{\mathcal{B}^2} \right) dt^2 + \frac{\mathcal{B}^2 + 3r^2}{\mathcal{B}^2 + r^2 + \beta \mathcal{F}(\mathcal{B}^2 + 3r^2)} dr^2 + r^2 d\theta^2 + r^2 \sin^2 \theta d\vartheta^2. \quad (40)$$

The resulting state variables (the energy density and radial/tangential pressures) are

$$\begin{aligned} \check{\mu} = & \frac{1}{72(\varpi + 4\pi)(\mathcal{B}^2 + 3r^2)^2} \left[\frac{18\varpi(9\mathcal{B}^2 + 10r^2) + 432\pi(\mathcal{B}^2 + r^2)}{\varpi + 2\pi} \right. \\ & + \frac{\beta}{\pi(\mathcal{B}^2 + 2r^2)^2} \left\{ 3(\varpi + 4\pi)\mathcal{B}^{10}g^2 + (\varpi + 4\pi)\mathcal{B}^8(2g(26r^2g + 9) \right. \\ & - 27\mathcal{C}_1) + 3\mathcal{B}^6(\varpi r^2(4g(23r^2g + 8) - 75\mathcal{C}_1) - 4\pi(r^2(75\mathcal{C}_1 - 4g \\ & \times (23r^2g + 8)) + 9)) + 45\mathcal{B}^4r^2(\varpi r^2(2g(7r^2g + 3) - 15\mathcal{C}_1) + 4\pi \\ & \times (r^2(2g(7r^2g + 3) - 15\mathcal{C}_1) - 2)) + 2(\varpi + 4\pi)g(\mathcal{B}^2 + 3r^2)^2 \\ & \times (3\mathcal{B}^4 + 7\mathcal{B}^2r^2 + 6r^4)(\mathcal{B}^2g + 3) \ln(\mathcal{B}^2 + 3r^2) + 9\mathcal{B}^2r^4(\varpi r^2(g \\ & \times (73r^2g + 48) - 99\mathcal{C}_1) + 4\pi(r^2(g(73r^2g + 48) - 99\mathcal{C}_1) - 9)) + 54r^6 \\ & \left. \left. \times (\varpi r^2(g(5r^2g + 4) - 9\mathcal{C}_1) + 4\pi(r^2(g(5r^2g + 4) - 9\mathcal{C}_1) - 1)) \right\} \right], \end{aligned} \quad (41)$$

$$\begin{aligned} \check{P}_r = & \frac{1}{72\pi} \left[\frac{18\pi\varpi(3\mathcal{B}^2 + 2r^2)}{(\varpi + 2\pi)(\varpi + 4\pi)(\mathcal{B}^2 + 3r^2)^2} + \frac{\beta}{(\mathcal{B}^2 + 2r^2)(\mathcal{B}^2 + 3r^2)} \right. \\ & \times \left\{ (\mathcal{B}^2 + 3r^2) \left(\frac{36\pi}{\varpi + 4\pi} + 9\mathcal{C}_1(\mathcal{B}^2 + 3r^2) - g^2(\mathcal{B}^2 + 3r^2)^2 - 2g \right. \right. \\ & \times (\mathcal{B}^2 + 3r^2)(\mathcal{B}^2g + 3) \ln(\mathcal{B}^2 + 3r^2) - 6\mathcal{B}^2g \left. \left. \right) + 18g(\mathcal{B}^2 + r^2) \right. \\ & \left. \left. (\mathcal{B}^2 + 2r^2) \right\} \right], \end{aligned} \quad (42)$$

$$\check{P}_\perp = -\frac{1}{72\pi(\mathcal{B}^2 + 2r^2)(\mathcal{B}^2 + 3r^2)^2(\varpi + 2\pi)(\varpi + 4\pi)} \left[\beta(\varpi + 2\pi) \right]$$

$$\begin{aligned}
& \times (\varpi(\mathcal{B}^2 + 3r^2)(g^2(\mathcal{B}^2 + 3r^2)^3 - 12g(\mathcal{B}^4 + 3\mathcal{B}^2r^2 + 3r^4) - 9\mathcal{C}_1 \\
& \times (\mathcal{B}^2 + 3r^2)^2) + 4\pi(-9(\mathcal{B}^4(\mathcal{B}^2\mathcal{C}_1 + 1) + 3r^4(9\mathcal{B}^2\mathcal{C}_1 + 1) \\
& + 3\mathcal{B}^2r^2(3\mathcal{B}^2\mathcal{C}_1 + 1) + 27\mathcal{C}_1r^6) - 12g(\mathcal{B}^4 + 3\mathcal{B}^2r^2 + 3r^4)(\mathcal{B}^2 + 3r^2) \\
& + g^2(\mathcal{B}^2 + 3r^2)^4)) - 18\pi\varpi(\mathcal{B}^2 + 2r^2)(3\mathcal{B}^2 + 2r^2) + 2\beta g(\varpi + 2\pi) \\
& \times (\varpi + 4\pi)(\mathcal{B}^2 + 3r^2)^3(\mathcal{B}^2g + 3) \ln(\mathcal{B}^2 + 3r^2) \Big]. \tag{43}
\end{aligned}$$

The pressure anisotropy in this case becomes

$$\ddot{\Pi} = \frac{3r^2(1 - \beta)}{2(\varpi + 4\pi)(\mathcal{B}^2 + 3r^2)^2}, \tag{44}$$

which vanishes on account of $\beta = 1$. These equations represent our first analytic solution to the modified field equations for $\beta \in [0, 1]$. It is observed that the original anisotropic system is now transformed into an isotropic system (for $\beta = 1$). Consequently, the change in β from 0 to 1 follows the process of isotropization of the considered setup.

5 Complexity of Compact Sources

In this section, we are dealing with the complexity of static spherical source which was recently presented by Herrera [24]. Later, this definition was also extended to the case of non-static dissipative scenario [25]. The fundamental notion of this definition is that the structure coupled with uniform/isotropic fluid distribution considered to be the complexity-free. On the other hand, some scalars can be calculated from orthogonal splitting of the Riemann tensor, one of them is Υ_{TF} that involves inhomogeneous/anisotropic factors, and thus adopted as the complexity factor. We extend Herrera's definition [24] to $f(\mathbb{R}, \mathbb{T})$ theory to explore the effects of modified corrections on the complexity. Consequently, Υ_{TF} becomes

$$\Upsilon_{TF}(r) = -\frac{4\pi}{r^3} \int_0^r y^3 \mu'(y) dy + 8\pi\Pi(\varpi + 1), \tag{45}$$

and the Tolman mass for this scenario can be specified as

$$m_T = 4\pi \int_0^r y^2 e^{\frac{(\chi+\sigma)}{2}} (\mu + 3P) dy, \tag{46}$$

which helps in determining the sphere's total energy. Combining the complexity factor (45) with Tolman mass, we obtain

$$m_T = \check{\mathcal{M}}_T \left(\frac{r}{\mathcal{R}} \right)^3 + r^3 \int_r^{\mathcal{R}} \frac{e^{\frac{(x+\sigma)}{2}}}{y} (\check{\mathbb{Y}}_{TF} - 8\pi\Pi\varpi) dy, \quad (47)$$

where $\check{\mathcal{M}}_T$ indicates the Tolman mass at the hypersurface.

As we have coupled two different sources, thus the factor $\check{\mathbb{Y}}_{TF}$ corresponding to the total distribution (10)-(12) comes out to be

$$\begin{aligned} \check{\mathbb{Y}}_{TF}(r) &= 8\pi\check{\Pi}(\varpi + 1) - \frac{4\pi}{r^3} \int_0^r y^3 \check{\mu}'(y) dy \\ &= 8\pi\Pi(\varpi + 1) - \frac{4\pi}{r^3} \int_0^r y^3 \mu'(y) dy \\ &+ 8\pi\Pi_{\mathfrak{B}}(\varpi + 1) + \frac{4\pi}{r^3} \int_0^r y^3 \mathfrak{B}_0^{0'}(y) dy, \end{aligned} \quad (48)$$

whose compact form is

$$\check{\mathbb{Y}}_{TF} = \mathbb{Y}_{TF} + \mathbb{Y}_{TF}^{\mathfrak{B}}, \quad (49)$$

where \mathbb{Y}_{TF} and $\mathbb{Y}_{TF}^{\mathfrak{B}}$ associate with the seed (19)-(21) and additional source (22)-(24), respectively. The solution (41)-(44) is established for the constraint $\check{\Pi} = 0$ that assists Eq.(48) to yield

$$\check{\mathbb{Y}}_{TF} = -\frac{4\pi}{r^3} \int_0^r y^3 \check{\mu}'(y) dy, \quad (50)$$

representing the complexity factor of geometry (40). Its value in terms of the field equations is casted as

$$\begin{aligned} \check{\mathbb{Y}}_{TF} &= -\frac{1}{216r^3(\varpi + 2\pi)(\varpi + 4\pi)} \left[\frac{1}{(\mathcal{B}^4 + 5\mathcal{B}^2r^2 + 6r^4)^2} \left\{ 48(\varpi + 2\pi)\beta r^5 \right. \right. \\ &\times (4\pi(\mathcal{B}^4(\mathcal{B}^2g(4\mathcal{B}^2g - 3) + 18) + 9gr^6(7\mathcal{B}^2g + 6) + 9r^4(\mathcal{B}^2g(7\mathcal{B}^2g + 9) \\ &+ 3) + 9\mathcal{B}^2r^2(\mathcal{B}^2g(3\mathcal{B}^2g + 2) + 6) + 27g^2r^8) + \varpi g(\mathcal{B}^6(4\mathcal{B}^2g - 3) + 9\mathcal{B}^4 \\ &\times r^2(3\mathcal{B}^2g + 2) + 9r^6(7\mathcal{B}^2g + 6) + 9\mathcal{B}^2r^4(7\mathcal{B}^2g + 9) + 27gr^8) - \mathcal{B}^2g \\ &\times (\varpi + 4\pi)(\mathcal{B}^2g + 3)(\mathcal{B}^2 + 3r^2)^2 \ln(\mathcal{B}^2 + 3r^2)) - 36\pi(\mathcal{B}^2 + 2r^2)^2 \\ &\left. \times \left(3\varpi r(\mathcal{B}^4 + 5\mathcal{B}^2r^2 + 40r^4) - \sqrt{3}\varpi\sqrt{\mathcal{B}^2}(\mathcal{B}^2 + 3r^2)^2 \tan^{-1}\left(\frac{\sqrt{3}r}{\sqrt{\mathcal{B}^2}}\right) \right) \right\} \end{aligned}$$

$$\left. + 288\pi r^5 \right\} + \frac{216(\varpi + 2\pi)(\varpi + 4\pi)\mathcal{B}^2\beta\mathcal{C}_1 r^5}{(\mathcal{B}^2 + 2r^2)^2} \Big]. \quad (51)$$

5.1 Two Systems possessing the Same Complexity Factor

Here, the newly added source $\mathfrak{B}_{\eta\zeta}$ is assumed to be complexity-free, i.e., $\mathbb{Y}_{TF}^{\mathfrak{B}} = 0$, thus its insertion in the seed source does not affect the corresponding \mathbb{Y}_{TF} and hence leading to $\check{\mathbb{Y}}_{TF} = \mathbb{Y}_{TF}$ or

$$8\pi\Pi_{\mathfrak{B}}(\varpi + 1) = -\frac{4\pi}{r^3} \int_0^r y^3 \mathfrak{B}_0^{0'}(y) dy. \quad (52)$$

The right side together with Eq.(22) provides

$$-\frac{4\pi}{r^3} \int_0^r y^3 \mathfrak{B}_0^{0'}(y) dy = \frac{1}{r^2} \left(\mathcal{F} - \frac{r\mathcal{F}'}{2} \right), \quad (53)$$

which after substitution in Eq.(52) yields the differential equation as

$$\begin{aligned} & (\varpi + 1) \left\{ \mathcal{F}'(r) \left(\frac{\chi'}{4} + \frac{1}{2r} \right) + \mathcal{F}(r) \left(\frac{\chi''}{2} - \frac{1}{r^2} + \frac{\chi'^2}{4} - \frac{\chi'}{2r} \right) \right. \\ & \left. + e^{-\sigma} \left(\frac{\mathcal{G}''(r)}{2} + \frac{\mathcal{G}'(r)\chi'}{2} - \frac{\mathcal{G}'(r)\sigma'}{4} + \frac{\beta\mathcal{G}'(r)^2}{4} - \frac{\mathcal{G}'(r)}{2r} \right) \right\} \\ & - \frac{1}{2} \left(\frac{2\mathcal{F}(r)}{r^2} - \frac{\mathcal{F}'(r)}{r} \right) = 0. \end{aligned} \quad (54)$$

This is in terms of both the deformation functions, thus we again take $\mathcal{G}(r) = gr^2$ as used earlier to solve this for $\mathcal{F}(r)$. Equation (54) depends on unknown metric components describing the original source $\mathbb{T}_{\eta\zeta}$, thus we need to employ the Tolman IV ansatz to determine the solution. These components are

$$\chi(r) = \ln \left\{ \mathcal{A}^2 \left(1 + \frac{r^2}{\mathcal{B}^2} \right) \right\}, \quad (55)$$

$$\rho(r) = e^{-\sigma} = \frac{(\mathcal{B}^2 + r^2)(\mathcal{C}^2 - r^2)}{\mathcal{C}^2(\mathcal{B}^2 + 2r^2)}, \quad (56)$$

which produce the energy density (19) and isotropic pressure (P_r and P_{\perp} are equal in this case) as

$$\mu = \frac{1}{4\mathcal{C}^2(\mathcal{B}^2 + 2r^2)^2(\varpi + 2\pi)(\varpi + 4\pi)} [4(\varpi + 3\pi)\mathcal{B}^4 + \mathcal{B}^2]$$

$$\begin{aligned} & \times (8\varpi r^2 + 5\varpi \mathcal{C}^2 + 28\pi r^2 + 12\pi \mathcal{C}^2) + 2r^2 \{4\pi(3r^2 + \mathcal{C}^2) \\ & + \varpi(3r^2 + 2\mathcal{C}^2)\}, \end{aligned} \quad (57)$$

$$\begin{aligned} P = & \frac{1}{4\mathcal{C}^2(\mathcal{B}^2 + 2r^2)^2(\varpi + 2\pi)(\varpi + 4\pi)} [\mathcal{B}^2 \{4\pi(\mathcal{C}^2 - 5r^2) - 4\varpi r^2 \\ & + 3\varpi \mathcal{C}^2\} - 4\pi \mathcal{B}^4 + 2r^2 \{2\varpi \mathcal{C}^2 - 3\varpi r^2 - 4\pi(3r^2 - \mathcal{C}^2)\}]. \end{aligned} \quad (58)$$

Equations (34) and (35) provide two constants \mathcal{A}^2 and \mathcal{B}^2 , while we have \mathcal{C}^2 as

$$\mathcal{C}^2 = \frac{\mathcal{R}^3}{\mathcal{M}}. \quad (59)$$

Substituting the metric potentials (55) and (56) in (54), we have

$$\begin{aligned} \mathcal{F}(r) = & \frac{r^2(\mathcal{B}^2 + r^2)}{\mathcal{B}^2(2 + \varpi) + r^2(2\varpi + 3)} \left[\mathbb{C}_2 - \frac{g(1 + \varpi)}{8\mathcal{C}^2} \left\{ (\mathcal{B}^2 + 2\mathcal{C}^2) \right. \right. \\ & \times (\mathcal{B}^2 \beta g + 4) \ln(\mathcal{B}^2 + 2r^2) - 2r^2(\mathcal{B}^2 \beta g - 2\beta \mathcal{C}^2 g + 6) \\ & \left. \left. + \frac{2\mathcal{B}^2(\mathcal{B}^2 + 2\mathcal{C}^2)}{\mathcal{B}^2 + 2r^2} - 2\beta g r^4 \right\} \right], \end{aligned} \quad (60)$$

where \mathbb{C}_2 identifies as an integration constant. Hence, the temporal metric function is the same as given in Eq.(38) whereas the radial component has the form

$$\begin{aligned} e^\sigma = \rho^{-1} = & 8\mathcal{C}^2 \{(\varpi + 2)\mathcal{B}^2 + (2\varpi + 3)r^2\} \left[8(\mathcal{C}^2 - r^2) \{(\varpi + 2)\mathcal{B}^2 \right. \\ & + (2\varpi + 3)r^2\} + \beta r^2(\mathcal{B}^2 + r^2) \left\{ 8\mathcal{C}^2 \mathbb{C}_2 + g(1 + \varpi) \left(2r^2(\beta g \right. \right. \\ & \times (\mathcal{B}^2 - 2\mathcal{C}^2) + 6) - (\mathcal{B}^2 + 2\mathcal{C}^2)(\beta \mathcal{B}^2 g + 4) \ln(\mathcal{B}^2 + 2r^2) \\ & \left. \left. + 2\beta g r^4 - \frac{2\mathcal{B}^2(\mathcal{B}^2 + 2\mathcal{C}^2)}{\mathcal{B}^2 + 2r^2} \right) \right\} \right]^{-1}. \end{aligned} \quad (61)$$

Equation (48) offers the definition of $\check{\mathbb{Y}}_{TF}$ which in the current setup leads to

$$\begin{aligned} \check{\mathbb{Y}}_{TF} = \mathbb{Y}_{TF} = & \frac{\pi(\mathcal{B}^2 + 2\mathcal{C}^2)}{16r^3\mathcal{C}^2(\mathcal{B}^2 + 2r^2)^2(\varpi + 2\pi)(\varpi + 4\pi)} \left[6\varpi \mathcal{B}^4 r + 128\pi r^5 \right. \\ & \left. - 3\varpi \sqrt{2\mathcal{B}^2}(\mathcal{B}^2 + 2r^2)^2 \tan^{-1} \left(r \sqrt{\frac{2}{\mathcal{B}^2}} \right) + 64\varpi r^5 + 20\varpi \mathcal{B}^2 r^3 \right]. \end{aligned} \quad (62)$$

5.2 Generating Solutions with Zero Complexity

We now find the other solution by discussing the case in which the original source with complexity $\mathbb{Y}_{TF} \neq 0$ becomes free from complexity after the inclusion of an additional source. Therefore, the total fluid configuration has no complexity, i.e., $\check{\mathbb{Y}}_{TF} = 0$, which makes Eq.(49) in terms of Tolman IV components and $\mathcal{G}(r) = gr^2$ as

$$\begin{aligned}
& 8r\{r\mathcal{F}'(r) - 2\mathcal{F}(r)\} + \frac{1}{\mathcal{C}^2(\mathcal{B}^2 + r^2)^2(\mathcal{B}^2 + 2r^2)^2(\varpi + 2\pi)(\varpi + 4\pi)} \\
& \left[\pi(\mathcal{B}^2 + r^2)^2(\mathcal{B}^2 + 2\mathcal{C}^2) \left\{ \varpi \left(6\mathcal{B}^4 r + 20\mathcal{B}^2 r^3 - 3\sqrt{2\mathcal{B}^2}(\mathcal{B}^2 + 2r^2)^2 \right. \right. \right. \\
& \times \tan^{-1} \left(\frac{\sqrt{2}r}{\sqrt{\mathcal{B}^2}} \right) + 64r^5 \Big) + 128\pi r^5 \Big\} - 8(\varpi + 4\pi)(\varpi + 2\pi)(\varpi + 1) \\
& \times r\{\mathcal{C}^2(\mathcal{B}^2 + 2r^2)^2(2(\mathcal{B}^4 + 2\mathcal{B}^2 r^2 + 2r^4)\mathcal{F}(r) - r\mathcal{F}'(r)(\mathcal{B}^2 + r^2) \\
& \times (\mathcal{B}^2 + 2r^2)) + 2r^4 g(\mathcal{B}^2 + r^2)^2(\beta g(\mathcal{B}^2 + r^2)(\mathcal{B}^2 + 2r^2)(r^2 - \mathcal{C}^2) \\
& \left. \left. \left. + \mathcal{B}^4 + 4\mathcal{B}^2 r^2 - \mathcal{B}^2 \mathcal{C}^2 + 6r^4 - 4r^2 \mathcal{C}^2) \right\} \right] = 0, \tag{63}
\end{aligned}$$

which is the first order differential equation whose solution is

$$\begin{aligned}
\mathcal{F}(r) = & \frac{r^2(\mathcal{B}^2 + r^2)}{8\mathcal{C}^2(\varpi^2 + 6\pi\varpi + 8\pi^2)(\varpi\mathcal{B}^2 + 2\varpi r^2 + 2\mathcal{B}^2 + 3r^2)} \left[(2\pi + \varpi) \right. \\
& \times (4\pi + \varpi) \{ 8\mathbb{C}_3 \mathcal{C}^2 + 2(\varpi + 1)r^2 g(g\beta(\mathcal{B}^2 - 2\mathcal{C}^2) + 6) - g(\varpi + 1) \\
& \times (\mathcal{B}^2 + 2\mathcal{C}^2) \ln(\mathcal{B}^2 + 2r^2)(\mathcal{B}^2 g\beta + 4) + 2(\varpi + 1)\beta r^4 g^2 \} + \frac{2\pi\varpi}{r^2} \\
& \times (\mathcal{B}^2 + 2\mathcal{C}^2) - \frac{2(\mathcal{B}^2 + 2\mathcal{C}^2)}{(\mathcal{B}^2 + 2r^2)} \{ 6\pi\varpi((\varpi + 1)\mathcal{B}^2 g - 1) + (\varpi + 1) \\
& \times \varpi^2 \mathcal{B}^2 g + 8\pi^2((\varpi + 1)\mathcal{B}^2 g - 2) \} - \frac{1}{r^3} \left\{ \pi\varpi\sqrt{2\mathcal{B}^2}(\mathcal{B}^2 + 2\mathcal{C}^2) \right. \\
& \left. \times \tan^{-1} \left(r\sqrt{\frac{2}{\mathcal{B}^2}} \right) \right\} \Big], \tag{64}
\end{aligned}$$

where \mathbb{C}_3 refers to an integration constant with dimension $\frac{1}{l^2}$. Henceforth, the corresponding deformed radial metric coefficient can be obtained as

$$e^\sigma = \rho^{-1} = \frac{\mathcal{C}^2(\mathcal{B}^2 + 2r^2)}{(\mathcal{B}^2 + r^2)(\mathcal{C}^2 - r^2) + \beta\mathcal{C}^2\mathcal{F}(r)(\mathcal{B}^2 + 2r^2)}. \tag{65}$$

Finally, the second solution for the constraint $\check{Y}_{TF} = 0$ is given as

$$\begin{aligned}
\check{\mu} = & \frac{1}{64\mathcal{C}^2(\varpi + 4\pi)(\varpi + 2\pi)} \left[\frac{16}{(\mathcal{B}^2 + 2r^2)^2} \{ 4(\varpi + 3\pi)\mathcal{B}^4 + \mathcal{B}^2(28\pi r^2 \right. \\
& + 8\varpi r^2 + 5\varpi\mathcal{C}^2 + 12\pi\mathcal{C}^2) + 2r^2(\varpi(3r^2 + 2\mathcal{C}^2) + 4\pi(3r^2 + \mathcal{C}^2)) \} \\
& - \frac{\beta}{\pi((\varpi + 2)\mathcal{B}^2 + (2\varpi + 3)r^2)^2} \left\{ 2r^2\varrho_1((\varpi + 2)\mathcal{B}^2 + (2\varpi + 3)r^2) \right. \\
& + 3\varrho_1(\mathcal{B}^2 + r^2)((\varpi + 2)\mathcal{B}^2 + (2\varpi + 3)r^2) - 2(2\varpi + 3)r^2\varrho_1(\mathcal{B}^2 + r^2) \\
& + \frac{1}{r^3(\mathcal{B}^2 + r^2)(\mathcal{B}^2 + 2r^2)^2((\varpi + 2)\mathcal{B}^2 + (2\varpi + 3)r^2)} \left(8r^5(\mathcal{B}^2 + 2\mathcal{C}^2) \right. \\
& \times ((\varpi + 1)\varpi^2\mathcal{B}^2g + 6\pi\varpi((\varpi + 1)\mathcal{B}^2g - 1) + 8\pi^2((\varpi + 1)\mathcal{B}^2g - 2)) \\
& - 4\pi\varpi r(\mathcal{B}^2 + 2r^2)^2(\mathcal{B}^2 + 2\mathcal{C}^2) - 2\pi\varpi\mathcal{B}^2r(\mathcal{B}^2 + 2r^2)(\mathcal{B}^2 + 2\mathcal{C}^2) \\
& + 3\sqrt{2\mathcal{B}^2}\pi\varpi(\mathcal{B}^2 + 2r^2)^2(\mathcal{B}^2 + 2\mathcal{C}^2) \tan^{-1} \left(r\sqrt{\frac{2}{\mathcal{B}^2}} \right) + 8r^5g(\varpi + 1) \\
& \times (\varpi + 2\pi)(\varpi + 4\pi)(\mathcal{B}^2 + 2r^2)(\mathcal{B}^2(2\beta r^2g - 2\beta g\mathcal{C}^2 + 1) + 2\beta r^4g \\
& \left. \left. + r^2(6 - 2\beta g\mathcal{C}^2) - 4\mathcal{C}^2) \right) \right\} \Bigg], \tag{66}
\end{aligned}$$

$$\begin{aligned}
\check{P}_r = & \frac{1}{64\mathcal{C}^2(\varpi + 2\pi)(\varpi + 4\pi)} \left[\frac{16}{(\mathcal{B}^2 + 2r^2)^2} \{ \mathcal{B}^2(4\pi(\mathcal{C}^2 - 5r^2) - 4\varpi r^2 \right. \\
& + 3\varpi\mathcal{C}^2) - 4\pi\mathcal{B}^4 + 2r^2(-3\varpi r^2 + 4\pi(\mathcal{C}^2 - 3r^2) + 2\varpi\mathcal{C}^2) \} \\
& + \frac{1}{\pi\beta(\varpi + 2\pi)(\varpi + 4\pi)(\mathcal{B}^2 + r^2)} \left\{ \frac{16g(\mathcal{C}^2 - r^2)}{\mathcal{B}^2 + 2r^2} + \varrho_1 \left(\frac{\mathcal{B}^2 + 3r^2}{\mathcal{B}^2 + r^2} \right) \right. \\
& \left. \times \frac{1}{(\varpi + 4\pi)(\varpi + 2\pi)((\varpi + 2)\mathcal{B}^2 + (2\varpi + 3)r^2)} \right\} \Bigg], \tag{67}
\end{aligned}$$

$$\begin{aligned}
\check{P}_\perp = & \frac{1}{128\mathcal{C}^2(\mathcal{B}^2 + 2r^2)^2(\varpi + 2\pi)(\varpi + 4\pi)} \left[32\{ \mathcal{B}^2(4\pi(\mathcal{C}^2 - 5r^2) \right. \\
& - 4\varpi r^2 + 3\varpi\mathcal{C}^2) - 4\pi\mathcal{B}^4 + 2r^2(4\pi(\mathcal{C}^2 - 3r^2) - 3\varpi r^2 + 2\varpi\mathcal{C}^2) \} \\
& + \frac{1}{\pi\beta(\mathcal{B}^2 + r^2)((\varpi + 2)\mathcal{B}^2 + (2\varpi + 3)r^2)^2} \left\{ 16(\varpi + 2\pi)(\varpi + 4\pi) \right. \\
& \times g(\mathcal{B}^2 + r^2)((\varpi + 2)\mathcal{B}^2 + (2\varpi + 3)r^2)^2(\mathcal{B}^4(-gr^4 + r^2(g\mathcal{C}^2 - 3) \\
& \left. + 2\mathcal{C}^2) + \mathcal{B}^2(-3r^6g + r^4(3g\mathcal{C}^2 - 10) + 7r^2\mathcal{C}^2) + 2r^6(g\mathcal{C}^2 - 5) \right.
\end{aligned}$$

$$\begin{aligned}
& - 2r^8g + 8r^4\mathcal{C}^2) + 2r^2\varrho_1(2\mathcal{B}^2 + r^2)(\mathcal{B}^2 + 2r^2)^2 + r^{-3}(\mathcal{B}^2 + r^2) \\
& \times (\mathcal{B}^2 + 2r^2)((\varpi + 2)\mathcal{B}^2 + (2\varpi + 3)r^2) \left(8r^5(\mathcal{B}^2 + 2\mathcal{C}^2)(\varpi^2\mathcal{B}^2 \right. \\
& \times g(\varpi + 1) + 6\pi\varpi((\varpi + 1)\mathcal{B}^2g - 1) + 8\pi^2((\varpi + 1)\mathcal{B}^2g - 2)) \\
& - 4\pi\varpi r(\mathcal{B}^2 + 2r^2)^2(\mathcal{B}^2 + 2\mathcal{C}^2) - 2\pi\varpi\mathcal{B}^2r(\mathcal{B}^2 + 2r^2)(\mathcal{B}^2 + 2\mathcal{C}^2) \\
& + 3\sqrt{2\mathcal{B}^2}\pi\varpi(\mathcal{B}^2 + 2r^2)^2(\mathcal{B}^2 + 2\mathcal{C}^2) \tan^{-1} \left(r\sqrt{\frac{2}{\mathcal{B}^2}} \right) + 8r^5g(\varpi + 1) \\
& \times (\varpi + 2\pi)(\varpi + 4\pi)(\mathcal{B}^2 + 2r^2)(\mathcal{B}^2(2\beta r^2g - 2\beta g\mathcal{C}^2 + 1) + 2\beta r^4g \\
& + r^2(6 - 2\beta g\mathcal{C}^2) - 4\mathcal{C}^2) \left. \right) - (\mathcal{B}^2 + 2r^2)^3(2(2\varpi + 3)r^2\varrho_1(\mathcal{B}^2 + r^2) \\
& - 2r^2\varrho_1((\varpi + 2)\mathcal{B}^2 + (2\varpi + 3)r^2) - 2\varrho_1(\mathcal{B}^2 + r^2)((\varpi + 2)\mathcal{B}^2 \\
& + (2\varpi + 3)r^2)) \left. \right\} \Big], \tag{68}
\end{aligned}$$

where ϱ_1 and the anisotropic factor for this solution are given in Appendix A.

6 Graphical Interpretation of the Obtained Solutions

The following differential equation interlinks mass and energy density of the sphere that can be solved numerically along with the condition $m(0) = 0$ to calculate mass as

$$\frac{dm(r)}{dr} = 4\pi r^2 \check{\mu}, \tag{69}$$

where $\check{\mu}$ is provided in Eqs.(41) and (66) with respect to each solution. The compactness of a geometrical structure primarily measures how intricate particles of that object are arranged, and we represent it as $\nu(r)$ in this case. The tightness of these particles can be determined by calculating compactness factor, which is also defined by the mass-radius ratio. It was observed to be less than $\frac{4}{9}$ by Buchdahl [38] for a spherical model. The noteworthy fact is that the wavelength of electromagnetic radiations in the neighborhood of a self-gravitating system is affected by its compactness. These radiations change their path from geodesic motion due to the gravitational attraction

of the compact object. Such radiations are then redshifted which can mathematically be determined as

$$z(r) = \{1 - 2\nu(r)\}^{-\frac{1}{2}} - 1, \quad (70)$$

whose maximum value is observed as 2 and 5.211 for perfect [38] and anisotropic fluids [39], respectively.

In the field of astrophysics, it is interesting to know whether a compact structure incorporates an ordinary matter or not. The presence of such a fluid and viability of the resulting model can be guaranteed by the fulfillment of energy conditions. On the other hand, if any of these bounds does not satisfy then there must be an exotic matter inside the system. They have the following form in the considered setup

$$\begin{aligned} \check{\mu} &\geq 0, & \check{\mu} + \check{P}_r &\geq 0, \\ \check{\mu} + \check{P}_\perp &\geq 0, & \check{\mu} - \check{P}_r &\geq 0, \\ \check{\mu} - \check{P}_\perp &\geq 0, & \check{\mu} + \check{P}_r + 2\check{P}_\perp &\geq 0. \end{aligned} \quad (71)$$

The obtained isotropic/anisotropic models which show stable behavior are considered as an important subject of discussion among all the celestial structures. Multiple techniques have been introduced in this regard to check the stability. Firstly, we use the causality condition according to which the inequalities $0 < v_{s\perp}^2 < 1$ and $0 < v_{sr}^2 < 1$ should be satisfied to get stable behavior [40]. Here,

$$v_{s\perp}^2 = \frac{d\check{P}_\perp}{d\check{\mu}}, \quad v_{sr}^2 = \frac{d\check{P}_r}{d\check{\mu}},$$

are the tangential and radial sound speeds, respectively. If the absolute value of the difference between both the sound speeds, i.e., $|v_{s\perp}^2 - v_{sr}^2|$ lies in the interval $(0, 1)$, then the solution must be stable, named as the Herrera cracking concept [41]. Lastly, the adiabatic index (Γ) is analyzed which states that the stable star must satisfy the inequality $\Gamma > \frac{4}{3}$ [42]. Here, $\check{\Gamma}$ in terms of effective energy density and pressure is given as

$$\check{\Gamma} = \frac{\check{\mu} + \check{P}_r}{\check{P}_r} \left(\frac{d\check{P}_r}{d\check{\mu}} \right). \quad (72)$$

We take a linear $f(\mathbb{R}, \mathbb{T})$ model (9) to explore deformation functions, the scalar Υ_{TF} and the effective state variables corresponding to different

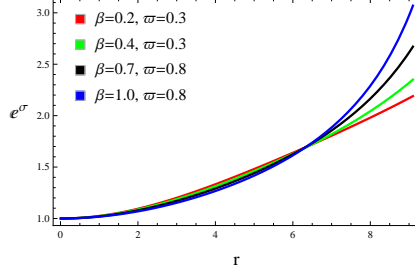


Figure 1: Deformed g_{rr} component (39) for the solution corresponding to $\check{\Pi} = 0$.

constraints through graphical analysis. We consider multiple choices of the decoupling and coupling parameters to study their role on physical attributes of a particular $4U1820 - 30$ model by fixing $\mathbb{C}_1 = 0.01$ and $g = 0.003$. Figure 1 manifests graphs of the deformed g_{rr} metric function (39) showing increasing and non-singular trend for $0 < r < \mathcal{R}$. The parameters governing the matter distribution (such as pressure and energy density) are required to be maximum, positive and finite at the center, and show linear decrement towards the boundary to meet acceptability criteria of the developed model. We observe acceptable behavior of our first solution (41)-(44) from Figure 2. The upper left plot shows that the effective energy density is maximum in the core. Further, it decreases by increasing both the parameters ϖ and β near the center, while shows opposite trend near the boundary. On the other hand, the pressure in both directions is observed to be in direct relation with ϖ as well as β . The vanishing of the radial pressure at $r = \mathcal{R}$ can also be seen from the upper right plot. We transform anisotropic system to an isotropic for $\beta = 1$ that can be confirmed from the last plot, as the anisotropy is zero throughout for that value. Moreover, this factor shows increasing behavior for the remaining values of β .

Figure 3 (upper left plot) reveals that the isotropic system is initially less massive than anisotropic analog, but exhibits counter consequence towards the hypersurface. The compactness and redshift are plotted in the upper right and lower plots, respectively which meet their required limits. All the energy bounds must be fulfilled due to positive nature of the state variables except dominant conditions ($\check{\mu} - \check{P}_r \geq 0$ and $\check{\mu} - \check{P}_\perp \geq 0$), thus they are needed to be checked. Figure 4 assures validity of these conditions, hence our first solution is physically viable. We check the stability by using three different

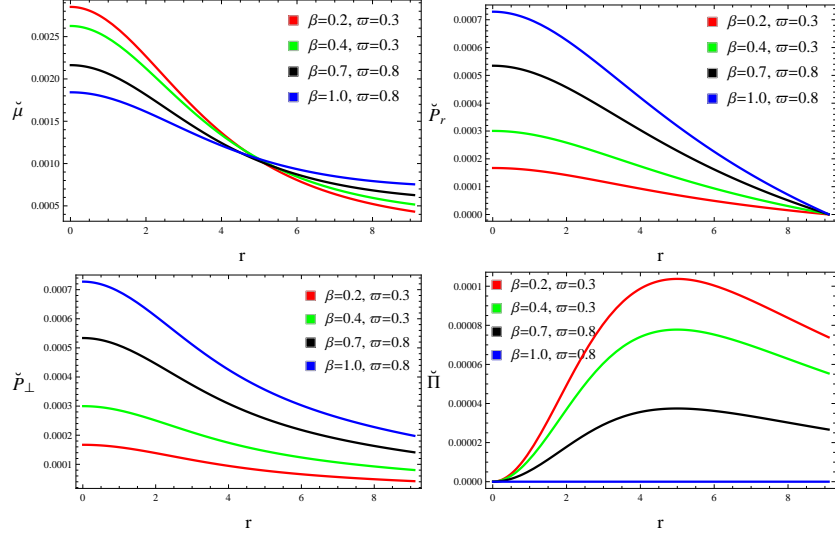


Figure 2: Matter variables and pressure anisotropy for the solution corresponding to $\tilde{\Pi} = 0$.

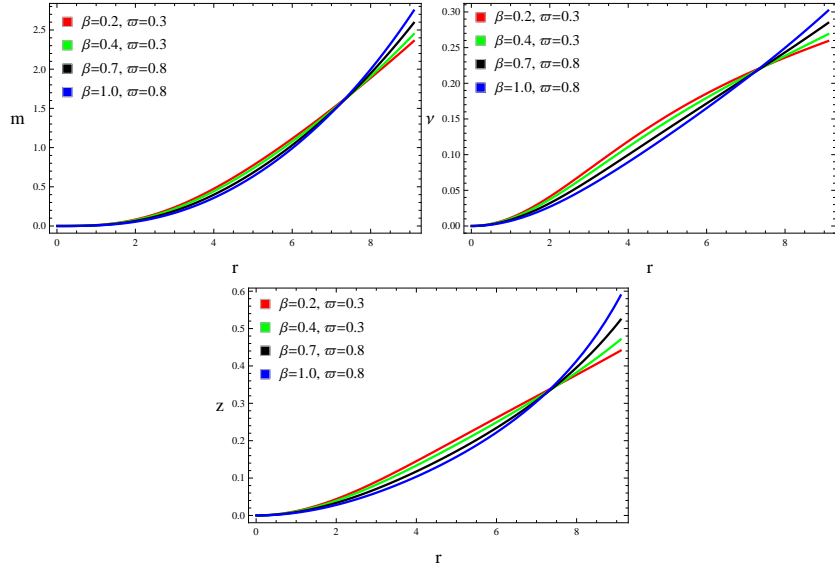


Figure 3: Mass, compactness and redshift for the solution corresponding to $\tilde{\Pi} = 0$.

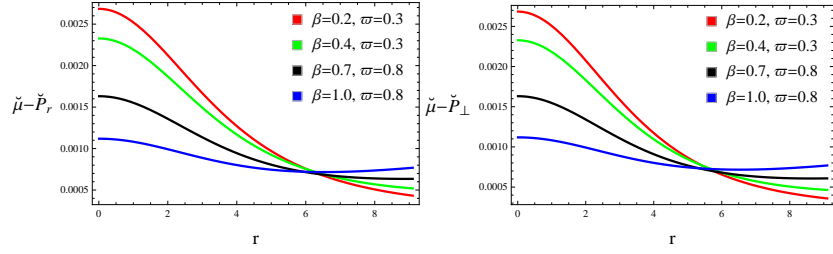


Figure 4: Dominant energy conditions for the solution corresponding to $\check{\Pi} = 0$.

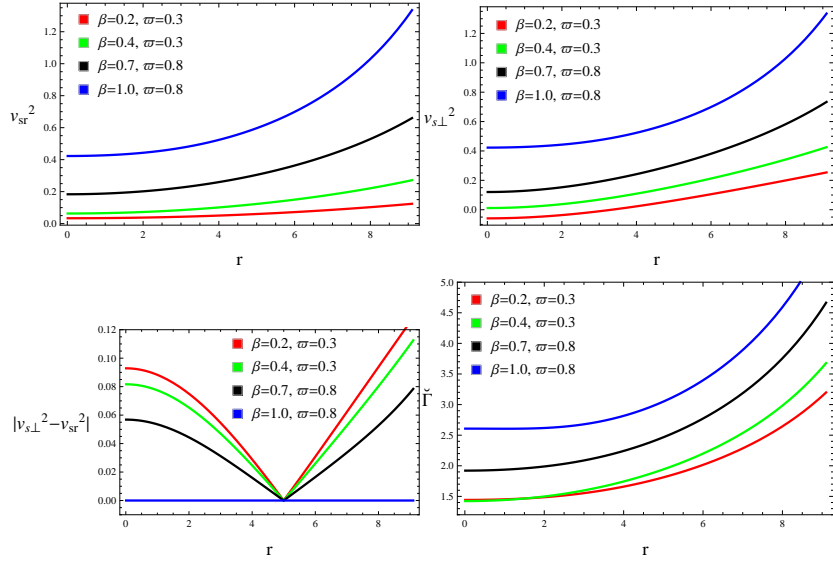


Figure 5: Radial/tangential velocities, $|v_{s\perp}^2 - v_{sr}^2|$ and adiabatic index for the solution corresponding to $\check{\Pi} = 0$.

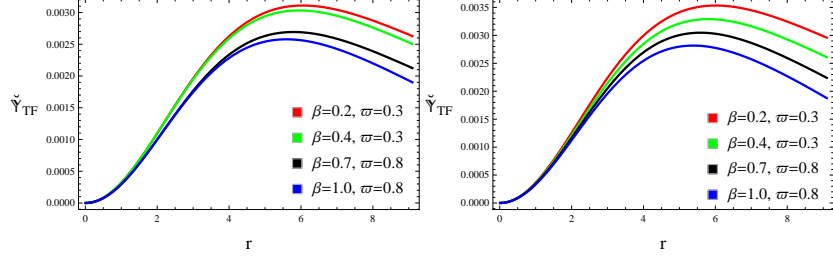


Figure 6: Complexity factors (51) and (62).

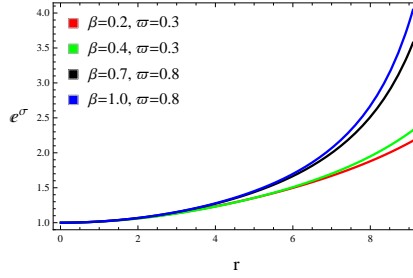


Figure 7: Deformed g_{rr} component (65) for the solution corresponding to $\check{Y}_{TF} = 0$.

approaches in Figure 5. The developed model (41)-(44) is unstable near the center for $\beta = 0.2$ (upper left plot) as well as near the boundary for $\beta = 1$ (upper two plots), while becomes stable for all the remaining considered choices of ϖ and β . Meanwhile, the resulting solution is observed to be stable everywhere by using the adiabatic index and the cracking condition (lower two plots). Figure 6 indicates that the increment in both ϖ and β decreases the complexity factors (51) and (62) which follows that the impact of complexity in $f(\mathbb{R}, \mathbb{T})$ theory is much lesser than that of $\mathbb{G}\mathbb{R}$.

We adopt another constraint $\check{Y}_{TF} = 0$ and obtain the corresponding solution (66)-(68) whose physical characteristics are analyzed by choosing $\mathbb{C}_3 = 0.01$. Figure 7 provides the plot of deformed g_{rr} component presenting non-singular trend throughout. The matter variables and pressure anisotropy are analyzed in Figure 8 which show acceptable behavior as we have discussed earlier. The tangential pressure in this case is lesser than the radial component (except at the center), thus anisotropy appears to be negative throughout. Figure 9 (upper left) exhibits that the sphere becomes more massive by increasing both parameters ϖ and β , in contrast to the

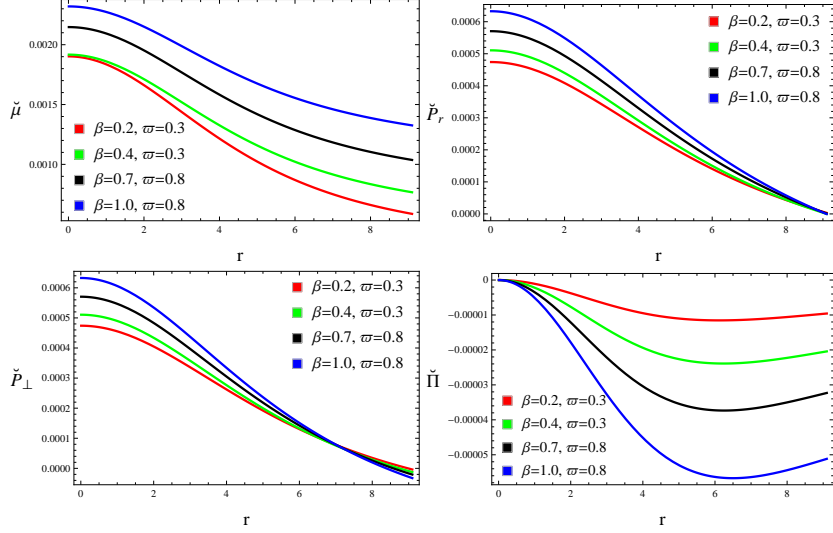


Figure 8: Matter variables and pressure anisotropy for the solution corresponding to $\check{Y}_{TF} = 0$.

result obtained through MGD. The right and lower plots confirm the acceptance of other two factors. Figure 10 discloses that our second solution as well as extended model (9) are also viable. Figure 11 reveals the stability of this solution everywhere.

7 Conclusions

The main objective of this paper is to extend some solutions for anisotropic self-gravitating distribution ($\mathbb{T}_{\eta\zeta}$) through the addition of an extra source ($\mathfrak{B}_{\eta\zeta}$) by employing gravitational decoupling scheme in $f(\mathbb{R}, \mathbb{T}) = \mathbb{R} + 2\varpi\mathbb{T}$ gravity. The corresponding field equations representing the total fluid configuration (seed and additional sources) have been formulated which are then split into two distinct sets by means of an EGD technique. Both sets of equations have ultimately represented their parent sources. For the first set describing seed source, we have taken the following metric potentials

$$\chi(r) = \ln \left\{ \mathcal{A}^2 \left(1 + \frac{r^2}{\mathcal{B}^2} \right) \right\}, \quad \rho(r) = e^{-\sigma(r)} = \frac{\mathcal{B}^2 + r^2}{\mathcal{B}^2 + 3r^2},$$

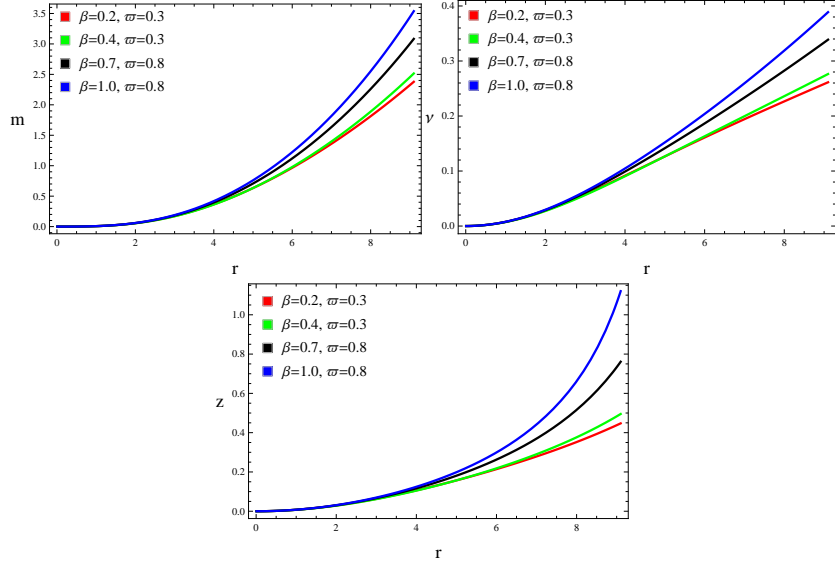


Figure 9: Mass, compactness and redshift for the solution corresponding to $\check{Y}_{TF} = 0$.

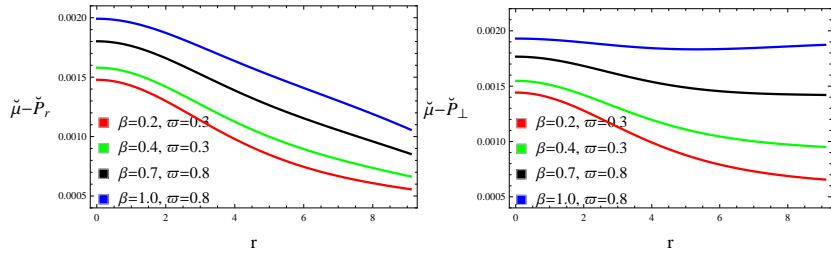


Figure 10: Dominant energy conditions for the solution corresponding to $\check{Y}_{TF} = 0$.

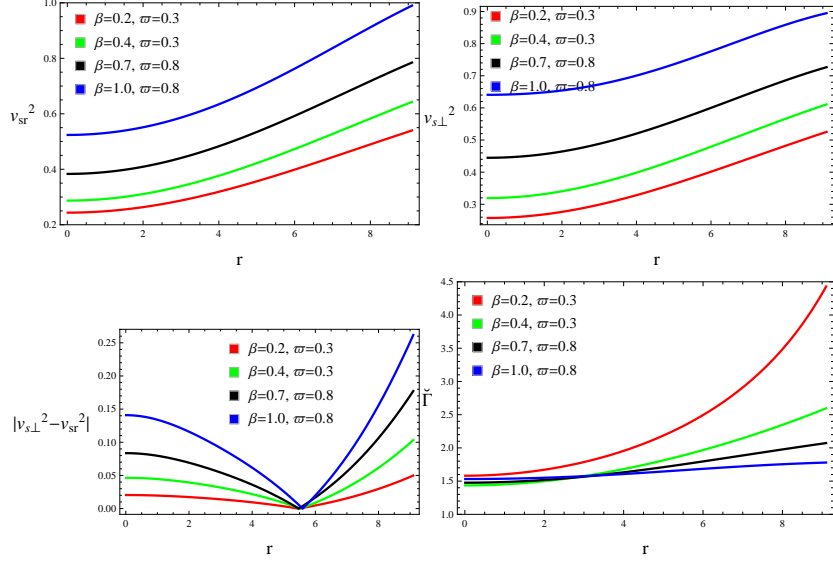


Figure 11: Radial/tangential velocities, $|v_{s\perp}^2 - v_{sr}^2|$ and adiabatic index for the solution corresponding to $\check{Y}_{TF} = 0$.

and the Tolman IV ansatz, resulting in two extended solutions. We have used the radius and mass of compact $4U1820 - 30$ model in order to determine three unknowns involving in these components. There have been five unknowns (\mathcal{F} , \mathcal{G} , \mathfrak{B}_{00} , \mathfrak{B}_{11} , \mathfrak{B}_{22}) incorporated in Eqs.(22)-(24), thus we required to implement two constraints simultaneously to get the solution. We have considered a particular form of $\mathcal{G}(r)$ along with two independent constraints leading to first and second solution. One constraint has been taken as disappearance of the effective anisotropy for $\beta = 1$, therefore the system becomes an isotropic for this value. We have then implemented another limitation on the complexity, i.e., the total setup has been considered to be the complexity-free.

The role of modified gravity and gravitational decoupling on physical attributes of the developed models have been explored by choosing $\varpi = 0.3, 0.8$ and $\beta = 0.2, 0.4, 0.7, 1$. The graphical interpretation of corresponding state determinants ((41)-(43) and (66)-(68)), anisotropic pressure ((44) and (A2)) and the energy constraints (71) have provided acceptable results for specific values of multiple constants. The redshift and compactness have also been shown to be within their required limits (Figures 3 and 9). We have ob-

served that the obtained model corresponding to $\check{\check{Y}}_{TF} = 0$ yields denser stellar structure, in comparison with the other solution. All the deformation functions have been found to be zero in the core of considered star and increasing towards the boundary. Further, the solution corresponding to $\check{\check{\Pi}}$ is stable throughout only for $\beta = 0.4, 0.7$ with causality condition, whereas the other solution is stable everywhere (Figures 5 and 11). The adiabatic index and Herrera's cracking concept have provided stable structures, thus our obtained solutions are compatible with those of GR [29]. The constraint $\check{\check{\Pi}} = 0$ has also been used in the the Brans-Dicke scenario to get solution which shows inconsistent behavior with $f(\mathbb{R}, \mathbb{T})$ gravity, as $\beta = 1$ provides unstable system in this case [31]. Finally, $\varpi = 0$ reduces all of our results to GR.

Appendix A

The value of ϱ_1 appearing in Eqs.(66)-(68) is

$$\begin{aligned} \varrho_1 = & (\varpi + 2\pi)(\varpi + 4\pi) \{ 2(\varpi + 1)r^2g(\beta g(\mathcal{B}^2 - 2\mathcal{C}^2) + 6) - (\varpi + 1)g \\ & \times (\mathcal{B}^2 + 2\mathcal{C}^2) \ln(\mathcal{B}^2 + 2r^2)(\mathcal{B}^2\beta g + 4) + 8\mathcal{C}_3\mathcal{C}^2 + 2(\varpi + 1)\beta r^4g^2 \} \\ & + \frac{2\pi\varpi(\mathcal{B}^2 + 2\mathcal{C}^2)}{r^2} - \frac{1}{(\mathcal{B}^2 + 2r^2)} \{ 2(\mathcal{B}^2 + 2\mathcal{C}^2)((\varpi + 1)\varpi^2\mathcal{B}^2g \\ & + 6\pi\varpi((\varpi + 1)\mathcal{B}^2g - 1) + 8\pi^2((\varpi + 1)\mathcal{B}^2g - 2) \} - \frac{\pi\varpi\sqrt{2\mathcal{B}^2}}{r^3} \\ & \times (\mathcal{B}^2 + 2\mathcal{C}^2) \tan^{-1} \left(\frac{\sqrt{2}r}{\sqrt{\mathcal{B}^2}} \right). \end{aligned} \quad (\text{A1})$$

The anisotropy for our second solution (66)-(68) is

$$\begin{aligned} \check{\check{\Pi}} = & \frac{\beta}{8\pi} \left[\frac{2g(\mathcal{B}^2 + r^2)(r^2 - \mathcal{C}^2)}{\mathcal{C}^2(\mathcal{B}^2 + 2r^2)} + \frac{g}{\mathcal{C}^2(\mathcal{B}^2 + 2r^2)^2} \{ \mathcal{B}^4(r^2(g\mathcal{C}^2 - 3) \right. \\ & - r^4g + 2\mathcal{C}^2) + \mathcal{B}^2(-3r^6g + r^4(3g\mathcal{C}^2 - 10) + 7r^2\mathcal{C}^2) - 2r^8g \\ & \left. + 2r^6(g\mathcal{C}^2 - 5) + 8r^4\mathcal{C}^2 \} - \frac{2\mathcal{B}^2r^2 + \mathcal{B}^4 + 3r^4}{8(\mathcal{B}^2 + r^2) \{ (\varpi + 2)\mathcal{B}^2 + (2\varpi + 3)r^2 \}} \right] \\ & \times \left(\frac{\varrho_2}{\mathcal{C}^2(\varpi + 2\pi)(\varpi + 4\pi)} + 8\mathcal{C}_3 \right) + \{ 16(\varpi + 2\pi)(\varpi + 4\pi) \} \end{aligned}$$

$$\begin{aligned}
& \times (\mathcal{B}^2 + r^2)((\varpi + 2)\mathcal{B}^2 + (2\varpi + 3)r^2)\}^{-1}(\mathcal{B}^2 + 2r^2) \left\{ \mathcal{C}^2(16\mathcal{C}_3r^2 \right. \\
& \times ((\varpi + 2)\mathcal{B}^2 + (2\varpi + 3)r^2) - 16(2\varpi + 3)\mathcal{C}_3r^2(\mathcal{B}^2 + r^2) + 16\mathcal{C}_3 \\
& \times (\mathcal{B}^2 + r^2)((\varpi + 2)\mathcal{B}^2 + (2\varpi + 3)r^2))(\varpi^2 + 6\pi\varpi + 8\pi^2) - 2r^2 \\
& \times (2\varpi + 3)\varrho_2(\mathcal{B}^2 + r^2) + 2r^2\varrho_2((\varpi + 2)\mathcal{B}^2 + (2\varpi + 3)r^2) + 2\varrho_2 \\
& \times (\mathcal{B}^2 + r^2)((\varpi + 2)\mathcal{B}^2 + (2\varpi + 3)r^2) + r(\mathcal{B}^2 + r^2)((\varpi + 2)\mathcal{B}^2 \\
& + (2\varpi + 3)r^2) \left(4(\varpi + 1)(\varpi^2 + 6\pi\varpi + 8\pi^2)(\mathcal{B}^2\beta g - 2\beta g\mathcal{C}^2 + 6) \right. \\
& \times rg + 8\beta r^3g^2(\varpi + 1)(\varpi^2 + 6\pi\varpi + 8\pi^2) - \frac{4\pi\varpi(\mathcal{B}^2 + 2\mathcal{C}^2)}{r^3} \\
& - \frac{2\pi\varpi\mathcal{B}^2(\mathcal{B}^2 + 2\mathcal{C}^2)}{r^3(\mathcal{B}^2 + 2r^2)} + 3r^{-4}\sqrt{2\mathcal{B}^2}\pi\varpi(\mathcal{B}^2 + 2\mathcal{C}^2) \tan^{-1}\left(\frac{\sqrt{2}r}{\sqrt{\mathcal{B}^2}}\right) \\
& + 8r(\mathcal{B}^2 + 2\mathcal{C}^2)(\mathcal{B}^2 + 2r^2)^{-2}(6\pi\varpi((\varpi + 1)\mathcal{B}^2g - 1) + 8\pi^2((\varpi + 1) \\
& \times \mathcal{B}^2g - 2) + (\varpi + 1)\varpi^2\mathcal{B}^2g) - 4(\varpi + 1)(\mathcal{B}^2 + 2r^2)^{-1}(\mathcal{B}^2 + 2\mathcal{C}^2) \\
& \left. \left. \times rg(\varpi^2 + 6\pi\varpi + 8\pi^2)(\mathcal{B}^2\beta g + 4) \right) \right\} \Bigg], \tag{A2}
\end{aligned}$$

where

$$\begin{aligned}
\varrho_2 = & (\varpi + 2\pi)(\varpi + 4\pi) \{ 2(\varpi + 1)r^2g(\beta g(\mathcal{B}^2 - 2\mathcal{C}^2) + 6) + 2\beta g^2 \\
& \times (\varpi + 1)r^4 - (\varpi + 1)g(\mathcal{B}^2 + 2\mathcal{C}^2) \ln(\mathcal{B}^2 + 2r^2)(\mathcal{B}^2\beta g + 4) \} \\
& + \frac{2\pi\varpi(\mathcal{B}^2 + 2\mathcal{C}^2)}{r^2} - \frac{1}{(\mathcal{B}^2 + 2r^2)} \{ 2(\mathcal{B}^2 + 2\mathcal{C}^2)((\varpi + 1)\varpi^2\mathcal{B}^2g \\
& + 6\pi\varpi((\varpi + 1)\mathcal{B}^2g - 1) + 8\pi^2((\varpi + 1)\mathcal{B}^2g - 2)) \} - \frac{\pi\varpi\sqrt{2\mathcal{B}^2}}{r^3} \\
& \times (\mathcal{B}^2 + 2\mathcal{C}^2) \tan^{-1}\left(\frac{\sqrt{2}r}{\sqrt{\mathcal{B}^2}}\right). \tag{A3}
\end{aligned}$$

References

- [1] Nojiri, S. and Odintsov, S.D.: Phys. Rep. **505**(2011)59; Capozziello, S. et al.: Class. Quantum Grav. **25**(2008) 085004; Nojiri, S. et al.: Phys. Lett. B **681**(2009)74.

- [2] Capozziello, S. et al.: *Mon. Not. R. Astron. Soc.* **394**(2009)947; de Felice, A. and Tsujikawa, S.: *Living Rev. Relativ.* **13**(2010)3.
- [3] Sharif, M. and Kausar, H.R.: *J. Cosmol. Astropart. Phys.* **07**(2011)022; Sharif, M. and Yousaf, Z.: *Astrophys. Space Sci.* **354**(2014)471.
- [4] Astashenok, A.V., Capozziello, S. and Odintsov, S.D.: *J. Cosmol. Astropart. Phys.* **01**(2015)001; *Phys. Lett. B* **742**(2015)160.
- [5] Bertolami, O. et al.: *Phys. Rev. D* **75**(2007)104016.
- [6] Harko, T. et al.: *Phys. Rev. D* **84**(2011)024020.
- [7] Deng, X.M. and Xie, Y.: *Int. J. Theor. Phys.* **54**(2015)1739.
- [8] Houndjo, M.J.S.: *Int. J. Mod. Phys. D* **21**(2012)1250003.
- [9] Das, A. et al.: *Phys. Rev. D* **95**(2017)124011.
- [10] Deb, D. et al.: *Phys. Rev. D* **97**(2018)084026.
- [11] Sharif, M. and Siddiqa, A.: *Eur. Phys. J. Plus* **133**(2018)226; Sharif, M. and Nawazish, I.: *Astrophys. Space Sci.* **363**(2018)67; Sharif, M. and Naseer, T.: *Eur. Phys. J. Plus* **137**(2022)1304.
- [12] Rej, P., Bhar, Piyali. and Govender, M.: *Eur. Phys. J. C* **81**(2021)316; Zubair, M. et al.: *New Astron.* **88**(2021)101610; Azmat, H. and Zubair M.: *Eur. Phys. J. Plus* **136**(2018)112.
- [13] Ovalle, J.: *Phys. Rev. D* **95**(2017)104019.
- [14] Ovalle, J. et al.: *Eur. Phys. J. C* **78**(2018)960.
- [15] Sharif, M. and Sadiq, S.: *Eur. Phys. J. C* **78**(2018)410.
- [16] Sharif, M. and Saba, S.: *Eur. Phys. J. C* **78**(2018)921; *Chin. J. Phys.* **59**(2019)481; Sharif, M. and Waseem, A.: *Ann. Phys.* **405**(2019)14.
- [17] Estrada, M. and Tello-Ortiz, F.: *Eur. Phys. J. Plus* **133**(2018)453.
- [18] Hensh, S. and Stuchlík, Z.: *Eur. Phys. J. C* **79**(2019)834.
- [19] Ovalle, J.: *Phys. Lett. B* **788**(2019)213.

- [20] Contreras, E. and Bargueño, P.: *Class. Quantum Grav.* **36**(2019)215009.
- [21] Sharif, M. and Ama-Tul-Mughani, Q.: *Ann. Phys.* **415**(2020)168122 ; Sharif, M. and Majid, A.: *Phys. Dark Universe* **30**(2020)100610; *ibid.* **32**(2021)100803; Sharif, M. and Aslam, M.: **81**(2021)641.
- [22] Zubair, M., Amin, M. and Azmat, H.: *Phys. Scr.* **96**(2021)125008.
- [23] Sharif, M. and Naseer, T.: *Chin. J. Phys.* **73**(2021)179; *Int. J. Mod. Phys. D* **31**(2022)2240017; *Phys. Scr.* **97**(2022)055004; *ibid.* **97**(2022)125016; *Pramana* **96**(2022)119; Naseer, T. and Sharif, M.: *Universe* **8**(2022)62.
- [24] Herrera, L.: *Phys. Rev. D* **97**(2018)044010.
- [25] Herrera, L., Di Prisco, A. and Ospino, J.: *Phys. Rev. D* **98**(2018)104059.
- [26] Yousaf, Z., Bhatti, M.Z. and Naseer, T.: *Eur. Phys. J. Plus* **135**(2020)353; *Phys. Dark Universe* **28**(2020)100535; *Int. J. Mod. Phys. D* **29**(2020)2050061; *Ann. Phys.* **420**(2020)168267.
- [27] Yousaf, Z. et al.: *Phys. Dark Universe* **29**(2020)100581; Yousaf, Z. et al.: *Mon. Not. R. Astron. Soc.* **495**(2020)4334; Sharif, M. and Naseer, T.: *Chin. J. Phys.* **77**(2022)2655; *Eur. Phys. J. Plus* **137**(2022)947.
- [28] Carrasco-Hidalgo, M. and Contreras, E.: *Eur. Phys. J. C* **81**(2021)757; Andrade, J. and Contreras, E.: *Eur. Phys. J. C* **81**(2021)889; Arias, C. et al.: *Ann. Phys.* **436**(2022)168671.
- [29] Casadio, R. et al.: *Eur. Phys. J. C* **79**(2019)826.
- [30] Maurya, S.K. and Nag, R.: *Eur. Phys. J. C* **82**(2022)48; Maurya, S.K. et al.: *Eur. Phys. J. C* **82**(2022)100.
- [31] Sharif, M. and Majid, A.: *Eur. Phys. J. Plus* **137**(2022)114.
- [32] Houndjo, M.J.S. and Piattella, O.F.: *Int. J. Mod. Phys. D* **2**(2012)1250024.
- [33] Moraes, P.H.R.S., Correa, R.A.C. and Ribeiro, G.: *Eur. Phys. J. C* **78**(2018)192.

- [34] Einstein, A.: Ann. Math. **40**(1939)922.
- [35] Clifton, T., Dunsby, P., Goswami, R. and Nzioki, A.M.: Phys. Rev. D **87**(2013)063517.
- [36] Goswami, R., Nzioki, A.M., Maharaj, S.D. and Ghosh, S.G.: Phys. Rev. D **90**(2014)084011.
- [37] Güver, T., Wroblewski, P., Camarota, L. and Özel, F.: Astrophys. J. **719**(2010)1807.
- [38] Buchdahl, H.A.: Phys. Rev. **116**(1959)1027.
- [39] Ivanov, B.V.: Phys. Rev. D **65**(2002)104011.
- [40] Abreu, H., Hernandez, H. and Nunez, L.A.: Class. Quantum Gravit. **24**(2007)4631.
- [41] Herrera, L.: Phys. Lett. A **165**(1992)206.
- [42] Heintzmann, H. and Hillebrandt, W.: Astron. Astrophys. **38**(1975)51.